

有关量子相变、冷原子、玻色-爱因斯坦凝聚体（**BEC**）的若干问题与进展

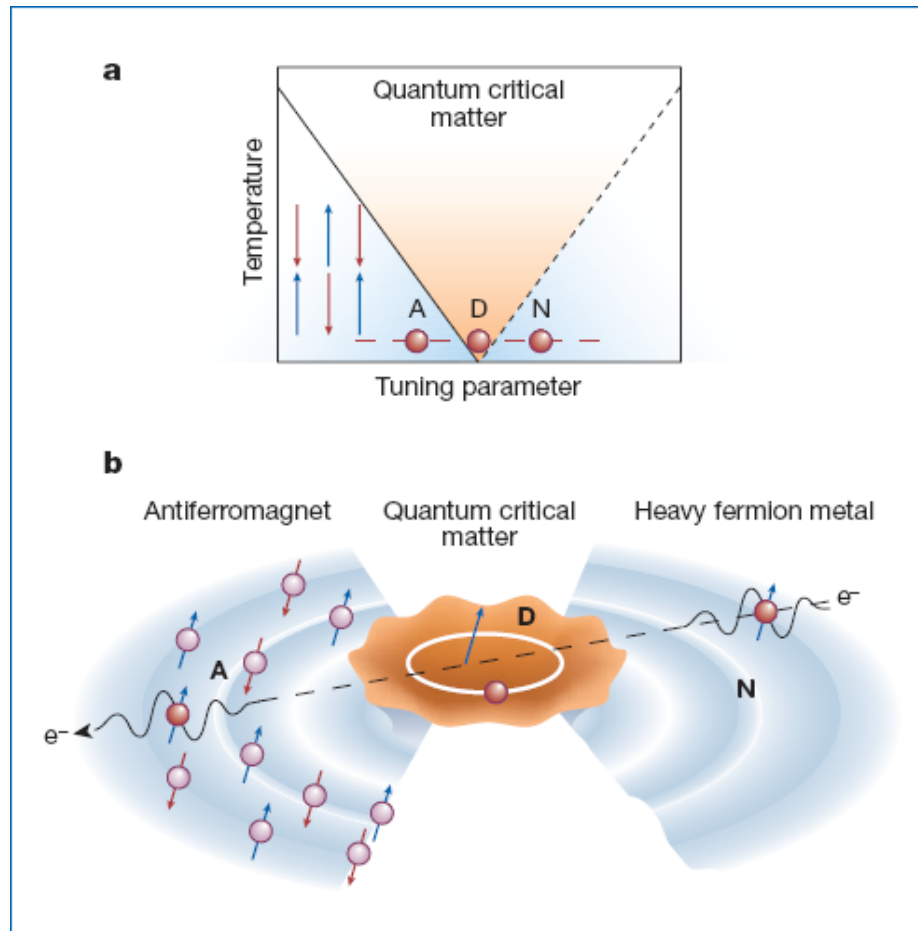
王文阁

中国科技大学，近代物理系

合作者:

秦品权，何乐为，王评，杨寅彪

(I) 量子相变 Quantum phase transition (QPT)



Coleman and Schofield, Nature 433, 226 (2005).

Figure 2 Schematic illustration of a quantum critical point showing the phase diagram (a) and the growth of droplets of quantum critical matter near the quantum critical point (b). **a**, Schematic phase diagram near a quantum critical point. Quantum critical points distort the fabric of the phase diagram creating a 'V-shaped' phase of quantum critical matter fanning out to finite temperatures from the quantum critical point. **b**, As matter is tuned to quantum criticality, ever-larger droplets of nascent order develop. On length-scales greater than these droplets, electrons propagate as waves. Inside the droplet, the intense fluctuations radically modify the motion of the electron, and may lead to it breaking up into its constituent spin and charge components. Physics inside the V-shaped region of the phase diagram (a) probes the interior of the quantum critical points (D), whereas the physics in the normal metal (N) or antiferromagnet (A) reflects their exterior. If, as we suspect, quantum critical matter is universal, then no information about the microscopic nature of the material penetrates into the droplets. Making an analogy with a black hole, the passage from non-critical, to critical quantum matter involves crossing a 'material event horizon'. Experiments that tune a material from the normal metal past a quantum critical point force electrons through the 'horizon' in the phase diagram, into the interior of the quantum critical matter, from which they ultimately re-emerge through a second horizon on the other side into a new universe of magnetically ordered matter.

量子相变定义

热相变：在有限温度下发生的相变，巨大的热涨落伴随其发生、为其发生的重要动因。

例子：液固相变，铁磁-顺磁相变。

量子相变：量子涨落起主要作用的相变。

为尽可能将量子涨落因素与热涨落因素区分开来，人们首先考虑零温、即基态情况。

研究量子相变的意义：为理解许多重要实验现象，比如有关高温超导、反铁磁膜、量子伊辛链等，提供重要、甚至是关键性的思路

狭义的量子相变定义

QPT

Non-analyticity of ground level
at critical point (临界点) λ_c

Drastic change of fundamental
properties of the ground state (GS),
when the parameter λ passes λ_c

Some low lying
excited states also
change drastically

量子相变的研究策略与方法

就其一般方法策略而言，

(a) 利用传统统计力学方法，计算系统在非零温下的配分函数，然后，令温度趋于零。

(b) 非传统方法（传统统计力学方法并不能揭示出量子相变点附近的所有性质）。例如，量子信息领域中的一些概念：纠缠度与保真度在许多系统中可以刻画量子相变的发生。

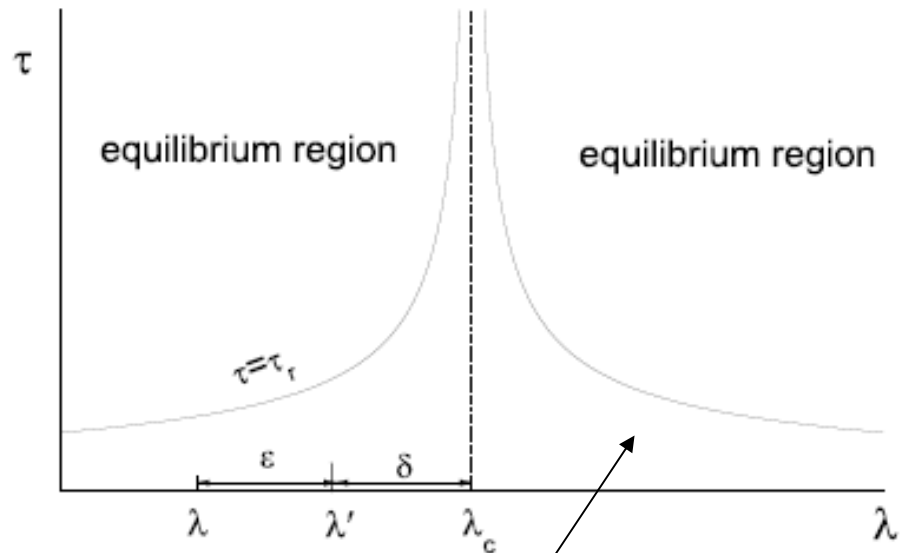
就与时间的关系而言，

(1) 有关平衡态的性质，包括对配分函数的计算，以及对定态的纠缠度和保真度的研究等。

(2) 有关非平衡态的性质，例如，对系统之动力学性质随时间变化的研究。

Equilibrium and non-equilibrium regions

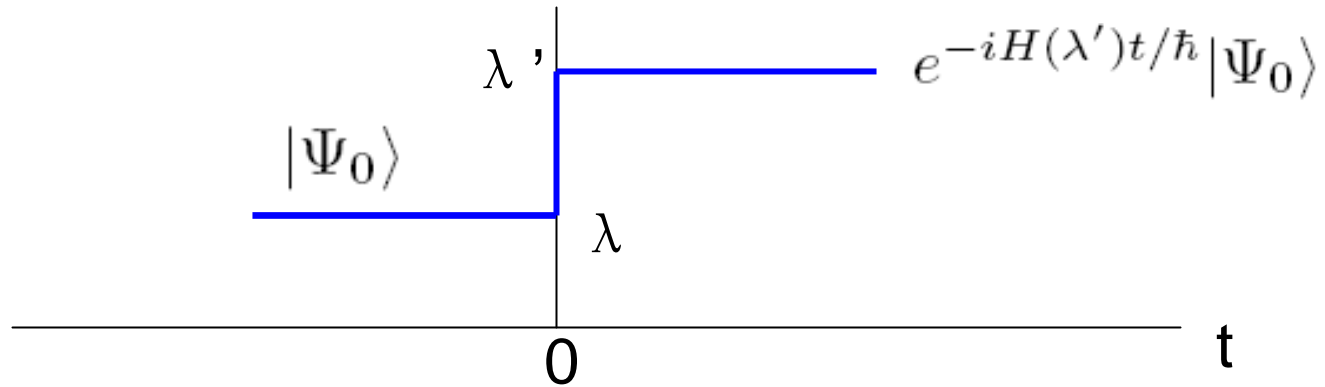
τ : time of interest
 τ_r : relaxation time.



Unitary dynamics should be considered

$$\epsilon = \lambda' - \lambda, \quad \delta = \lambda' - \lambda_c, \quad \Delta\lambda = \lambda - \lambda_c, \quad \eta = \epsilon / \Delta\lambda.$$

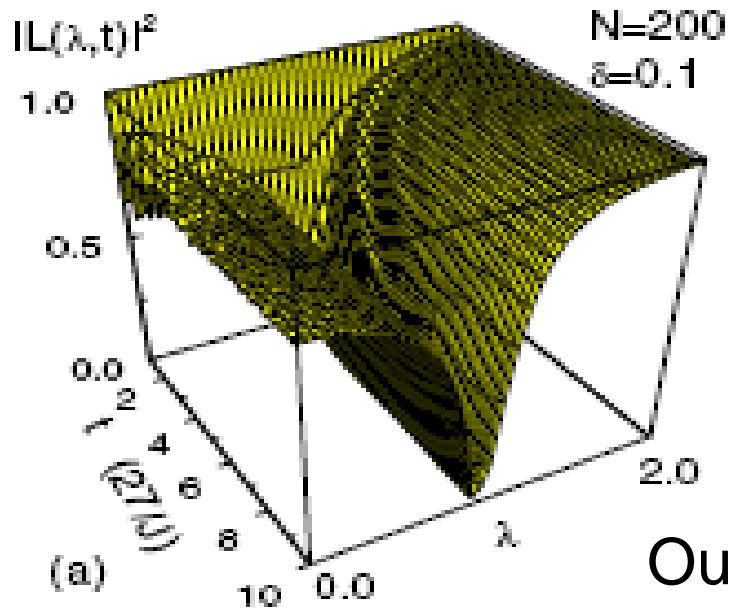
Survival probability (SP): in the non-equilibrium region



$|\Psi_0\rangle = |0_\lambda\rangle$: the GS of $H(\lambda)$

Survival probability

$$M(t) = |\langle \Psi_0 | e^{-iH(\lambda')t/\hbar} | \Psi_0 \rangle|^2$$



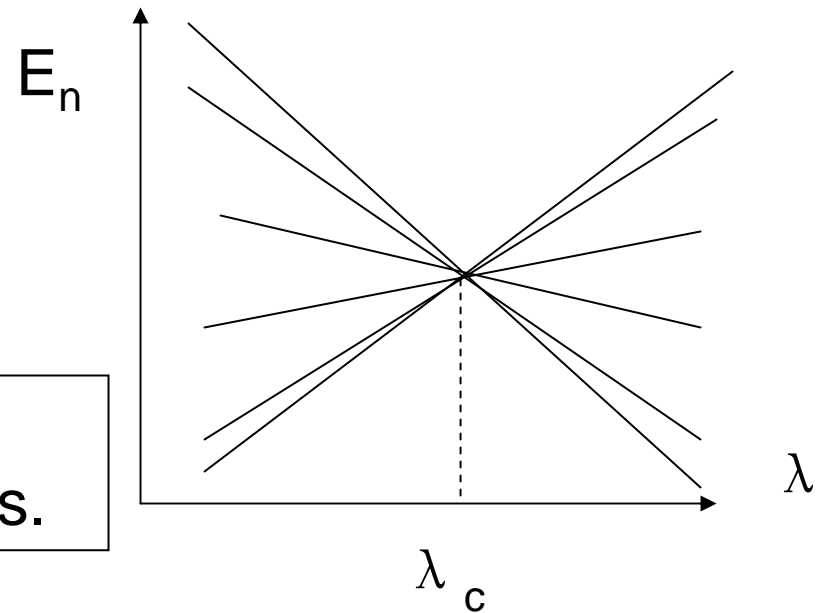
Our problem:

What is the decaying law of SP at QPT and whether it may reveal some characteristic properties of QPT?

A type of QPT that allows a semiclassical approach

The ground level has infinite degeneracy at the critical point

For example, due to avoided level crossings of infinite levels.



(1) Density of states at the ground level,
 $\rho(\lambda) \rightarrow \infty$ when $\lambda \rightarrow \lambda_c$.

For any fixed small value of $|\lambda - \lambda'|$, the overlap $|\langle 0_\lambda | 0_{\lambda'} \rangle|^2$ usually decreases significantly when λ' approaches λ_c .



$\bar{E} = \langle 0_\lambda | H(\lambda') | 0_\lambda \rangle$ may be in a relatively “high” energy region in the system $H(\lambda')$.



The semiclassical theory may be applicable in the study of the survival probability,

when λ' is sufficiently close to λ_c .

SP as a special case of quantum Loschmidt echo (Peres fidelity)

Quantum **Loschmidt echo** or (Peres) **fidelity** is a measure of the stability of quantum motion under small perturbation in the Hamiltonian,

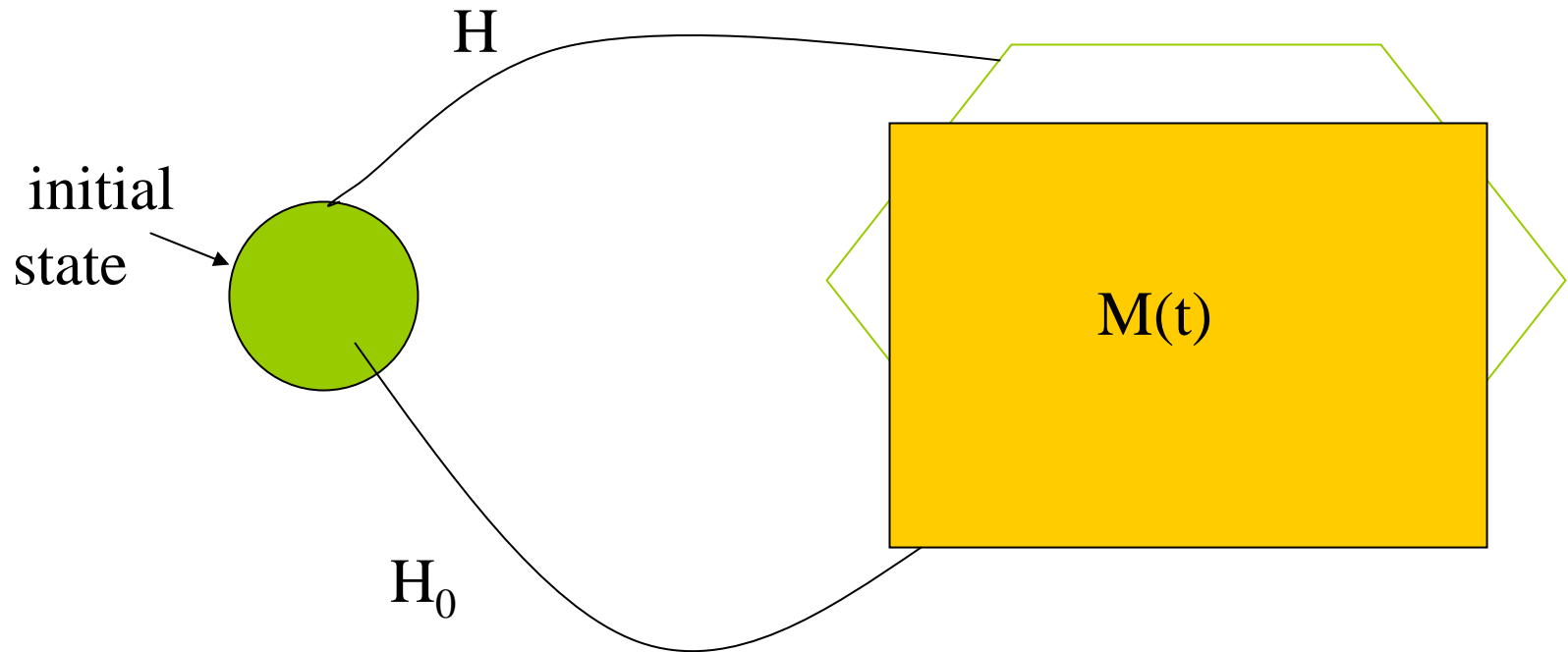
$$M_L(t) = |m(t)|^2$$

$$m(t) = \langle \Psi_0 | \exp(iH(\lambda')t/\hbar) \exp(-iH(\lambda)t/\hbar) | \Psi_0 \rangle.$$

For sufficiently small ϵ ,

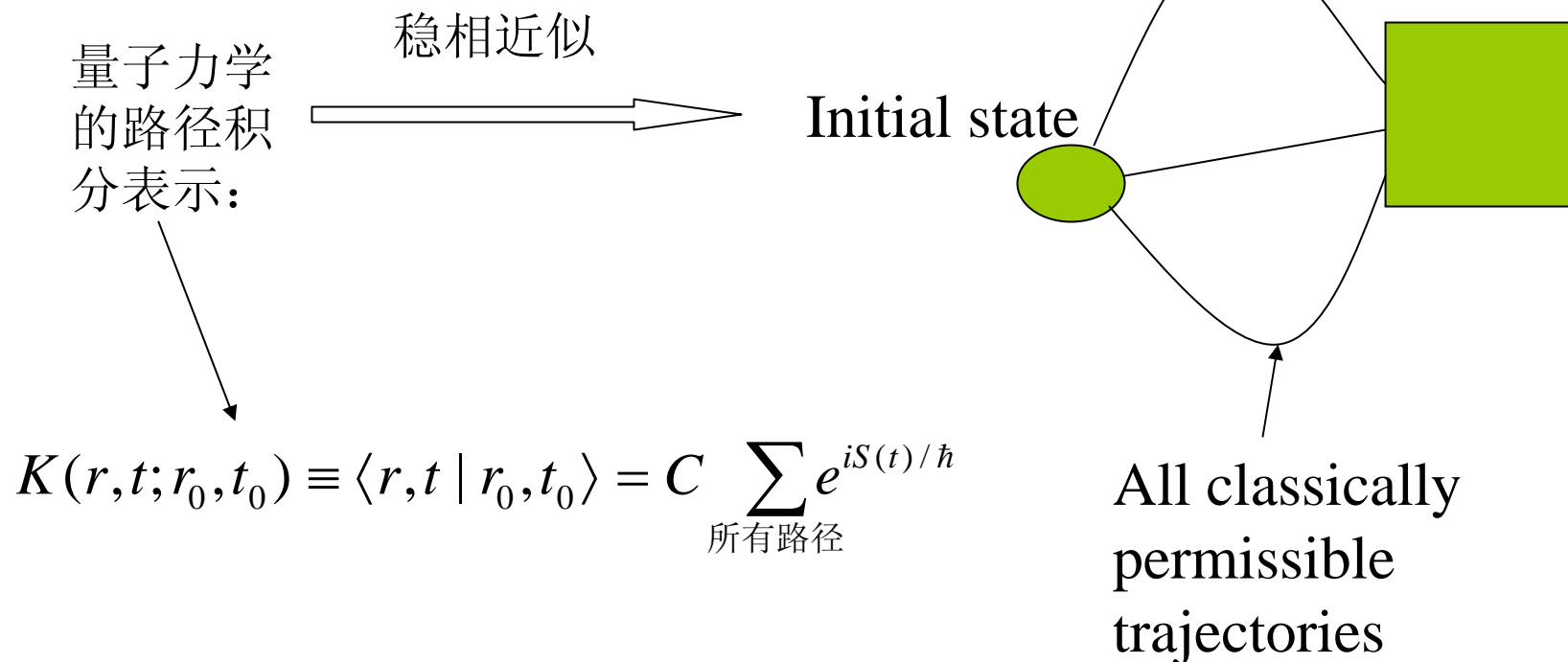
$$H(\lambda') \simeq H(\lambda) + \epsilon V, \text{ where } V = \frac{dH(\lambda)}{d\lambda}.$$

$m(t)$ is the overlap of the evolution of the same initial state under two slightly different Hamiltonians.



半经典理论的基本思路

An initial wave function in a d -dimensional configuration space, $\psi_0(\mathbf{r}_0)$, propagated by the semiclassical Van Vleck-Gutzwiller propagator,



波函数的半经典表示式

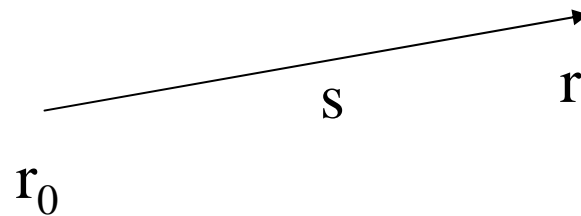
$$\psi_{\text{sc}}(\mathbf{r}; t) = \int d\mathbf{r}_0 K_{\text{sc}}(\mathbf{r}, \mathbf{r}_0; t) \psi_0(\mathbf{r}_0),$$

where $K_{\text{sc}}(\mathbf{r}, \mathbf{r}_0; t) = \sum_s K_s(\mathbf{r}, \mathbf{r}_0; t)$, with

$$K_s(\mathbf{r}, \mathbf{r}_0; t) = \frac{C_s^{1/2}}{(2\pi i \hbar)^{d/2}} \exp\left[\frac{i}{\hbar} S_s(\mathbf{r}, \mathbf{r}_0; t) - \frac{i\pi}{2} \mu_s \right].$$

$$S_s(\mathbf{r}, \mathbf{r}_0; t) = \int_0^t dt' \mathcal{L},$$

$$C_s = \left| \det(\partial^2 S_s / \partial r_{0i} \partial r_j) \right|$$



Consider an initial Gaussian wave packet centered at $\tilde{\mathbf{r}}_0$, with dispersion ξ and mean momentum $\tilde{\mathbf{p}}_0$,

$$\psi_0(\mathbf{r}_0) = \left(\frac{1}{\pi \xi^2} \right)^{d/4} \exp \left[\frac{i}{\hbar} \tilde{\mathbf{p}}_0 \cdot \mathbf{r}_0 - \frac{(\mathbf{r}_0 - \tilde{\mathbf{r}}_0)^2}{2\xi^2} \right].$$

For a ξ small enough,

$$m(t) \simeq m_{\text{sc1}}(t) \equiv \left(\frac{\xi^2}{\pi \hbar^2} \right)^{d/2} \int d\mathbf{r} \sum_s C_s \exp \left[\frac{i}{\hbar} \Delta S_s(\mathbf{r}, \tilde{\mathbf{r}}_0; t) - \frac{\xi^2}{\hbar^2} (\mathbf{p}_s - \tilde{\mathbf{p}}_0)^2 \right]$$

*R.A. Jalabert and H.M. Pastawski, Phys. Rev. Lett. **86**, 2490 (2001).*

$\Delta S_s(\mathbf{r}, \tilde{\mathbf{r}}_0; t) \simeq \epsilon \int_0^t dt' V[\mathbf{r}(t')]$ is the action difference along

nearby trajectories in the two systems.

M(t) expressed as an integral of \mathbf{p}_0

Changing variables $\mathbf{r} \rightarrow \mathbf{p}_0$,

$$m_{\text{sc}}(t) \simeq (\pi w^2)^{-d/2} \int d\mathbf{p}_0 \exp \left[\frac{i}{\hbar} \Delta S - \frac{(\mathbf{p}_0 - \tilde{\mathbf{p}}_0)^2}{w^2} \right]$$

$$\Delta S = \Delta S(\mathbf{p}_0, \tilde{\mathbf{r}}_0; t) \qquad w = \hbar / \xi$$

Loschmidt echo decay in regular systems with

In a very low energy region, the classical counterpart of the system (if exists) is usually a regular system.

The ground state has approximately a Gaussian shape.

(The main results to be derived do not depend on the Gaussian shape.)

$$(1) \quad d=1. \quad \Delta S \approx \varepsilon U t. \quad U=V|_{\text{initial point}} \quad \text{for } t \ll T$$

$$U = \frac{1}{T} \int_0^T V(t) dt \quad \text{for } t > T$$

T is the period of the classical motion.

d=1

WGW, G. Casati, and B. Li, *Phys. Rev. E* 75, 016201 (2007).

Expanding U to the second order term in p_0 ,

$$M_1(t) \simeq \frac{2c}{\sqrt{4 + (w^2\sigma\tilde{U}''t)^2}} \exp \left\{ \frac{-2(w\sigma\tilde{U}'t)^2}{4 + (w^2\sigma\tilde{U}''t)^2} \right\}$$

where $\sigma = \epsilon/\hbar$, $U' = \frac{\partial U}{\partial p_0}$, $U'' = \frac{\partial^2 U}{\partial p_0^2}$, $c \sim 1$ is a constant,
and tilde means evaluation at \tilde{p}_0

For short times, it has an initial Gaussian decay; for long times, it has a $1/t$ decay.

Very large d .

(2) For a very large d , there are many different frequencies, hence, T is very large and $\tau \ll T$.

For times of interest, the classical motion looks random due to the many different frequencies.

$$M_{\text{sc}}(t) \simeq \left| \int d\Delta S e^{i\Delta S/\hbar} P(\Delta S) \right|^2$$

where $P(\Delta S)$ is the distribution of ΔS and is close to a Gaussian distribution for times much shorter than T .

$$M_2(t) \simeq e^{-K_s \epsilon^2 t / \hbar^2} \text{ with } K_s \simeq \frac{1}{t} \langle [\int V dt]^2 - \langle \int V dt \rangle^2 \rangle$$

Similar to the chaotic case discussed in *N.R.Cerruti and S.Tomsovic, Phys. Rev.Lett.* **88**, 054103 (2002).

Summary of

semiclassical predictions for the decay law of SP at QPT.

For systems with classical counterparts in the very low energy region, the SP may have two qualitatively different decays for relatively long times:

Power law decay may appear for $d=1$.

Exponential decay for sufficiently large d .

Numerical study (1): single-mode Dicke model

Model: Interaction of a single bosonic mode and a collection of N two-level systems (collective motion).

$$H = \omega_0 J_z + \omega a^\dagger a + \frac{\lambda}{\sqrt{N}} (a^\dagger + a)(J_+ + J_-). \quad \hbar = 1$$

In the limit $N \rightarrow \infty$, the system undergoes a QPT at $\lambda_c = \frac{1}{2} \sqrt{\omega \omega_0}$, with a normal phase for $\lambda < \lambda_c$ and a super-radiant phase for $\lambda > \lambda_c$.

$$H(\lambda) = \sum_{k=1,2} e_{k\lambda} c_{k\lambda}^\dagger c_{k\lambda} + g$$

*C. Emary and T. Brandes, Phys. Rev. E **67**, 066203 (2003).*

Properties of Dicke model at QPT

In the normal phase,

$$e_{k\lambda}^2 = \frac{1}{2} \{ \omega^2 + \omega_0^2 + (-1)^k \sqrt{(\omega_0^2 - \omega^2)^2 + 16\lambda^2\omega\omega_0} \}$$

At the critical point,

$$e_{1\lambda_c} = 0 \text{ and } e_{2\lambda_c} = \sqrt{\omega^2 + \omega_0^2}.$$

Therefore, at the QPT, effectively the system has a classical counterpart with $d=1$.

$$e_{1\lambda} \simeq A |\Delta\lambda|^{1/2}$$

$$A = \frac{2(\omega\omega_0)^{3/4}}{\sqrt{\omega^2 + \omega_0^2}}$$

Properties of Dicke model at QPT

$$T \sim |\Delta\lambda|^{-\nu} \text{ with } \nu = 1/2.$$

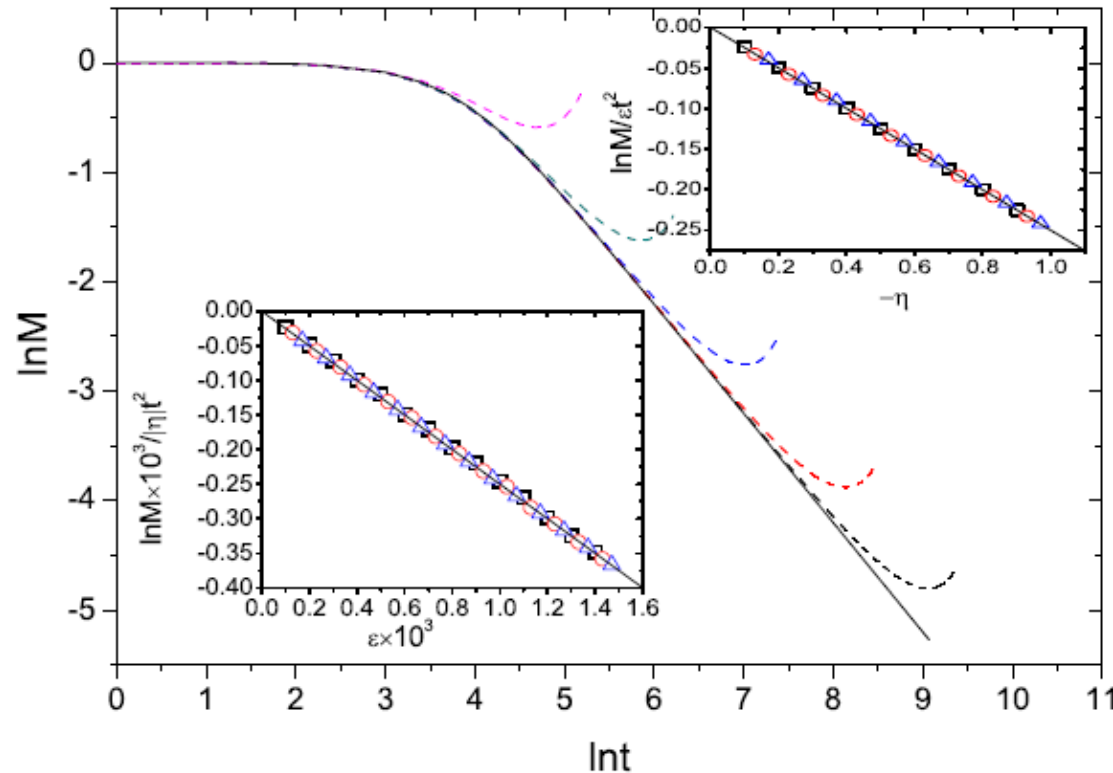
$$V_D = -\frac{A^2}{2e_{1\lambda}} \left(c_{1\lambda}^\dagger c_{1\lambda} + 2(c_{1\lambda}^\dagger)^2 + 2c_{1\lambda}^2 \right) \sim |\Delta\lambda|^{-1/2}$$

$$\Gamma \sim |\Delta\lambda|^{-1} \epsilon^2$$

$$M_1(t) \simeq \frac{2c}{\sqrt{4 + (w^2 \sigma \tilde{U}'' t)^2}} \exp \left\{ \frac{-2(w \sigma \tilde{U}' t)^2}{4 + (w^2 \sigma \tilde{U}'' t)^2} \right\}$$

Numerical results in Dicke model

$$\Gamma \sim |\Delta\lambda|^{-1} \epsilon^2$$



in the normal phase of Dicke model. Parameters $\omega = \omega_0 = 1$, $\epsilon = 10^{-3}$, and $\delta = -10^{-m}$ with $m = 4, 5, 6, 7, 8$ from top to bottom. The solid curve is a fitting curve of the form in Eq. (4), having a Gaussian decay followed by a $1/t$ decay.²⁴

Numerical study (2): 1-dimensional Ising chain

Model: A 1-dimensional Ising chain in a transverse field.

$$H(\lambda) = - \sum_{i=1}^N \sigma_i^z \sigma_{i+1}^z + \lambda \sigma_i^x.$$

Using Jordan-Wigner and Bogoliubov transformations, the Hamiltonian can be diagonalized,

$$H(\lambda) = \sum_k e_k (b_k^\dagger b_k - 1/2)$$

$$e_k = 2\sqrt{1 + \lambda^2 - 2\lambda \cos(ka)} \quad k = \frac{2\pi m}{aN}$$

with $m = -M, 1-M, \dots, M, N=2M+1$

Properties of Ising chain at QPT

In the large N limit, for fixed m (low energy region),

$$e_k = 2|\Delta\lambda| \qquad \lambda_c = 1$$

$$V_I = \frac{\lambda - \cos ka}{e_k/4} (b_k^\dagger b_k - \frac{1}{2}) + \frac{\sin ka}{e_k/2} i(b_k b_{-k} - b_k^\dagger b_{-k}^\dagger)$$

having no singularity.

Classical counterpart of Ising chain in low energy region

For $\lambda = \lambda_c$, large N , and relatively small m ,

$$e_k \simeq 4\pi|m|/N$$

Due to the linear dependence of e_k on m , the method of bosonization can be used to express the fermionic states

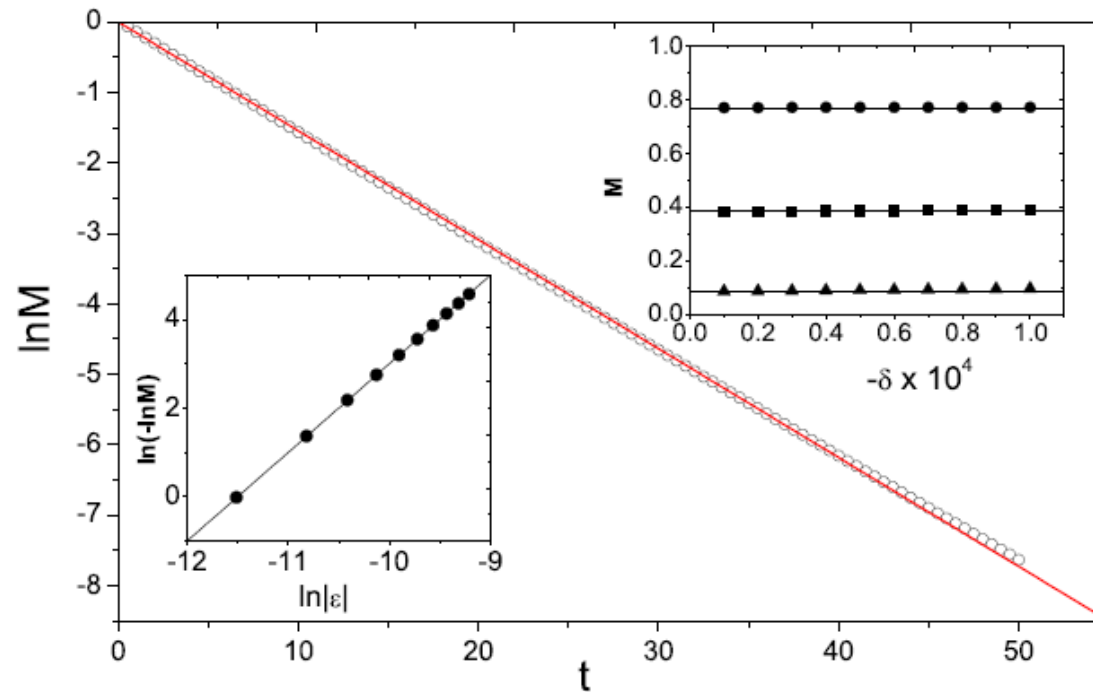
$$b_{k_1}^\dagger \dots b_{k_n}^\dagger |\text{vacuum}\rangle$$

in terms of bosonic modes.



The system has a classical counterpart with a large d in the low energy region.

Numerical results in Ising chain



$$M_2(t) \simeq e^{-K_s \epsilon^2 t / \hbar^2}$$

Two other models

(3) LMG model:

$$H = -\frac{1}{N}(S_x^2 + \gamma S_y^2) - \lambda S_z \quad \lambda_c = 1$$

$d=1$ and power law decay $1/t$ of the SP has been found.

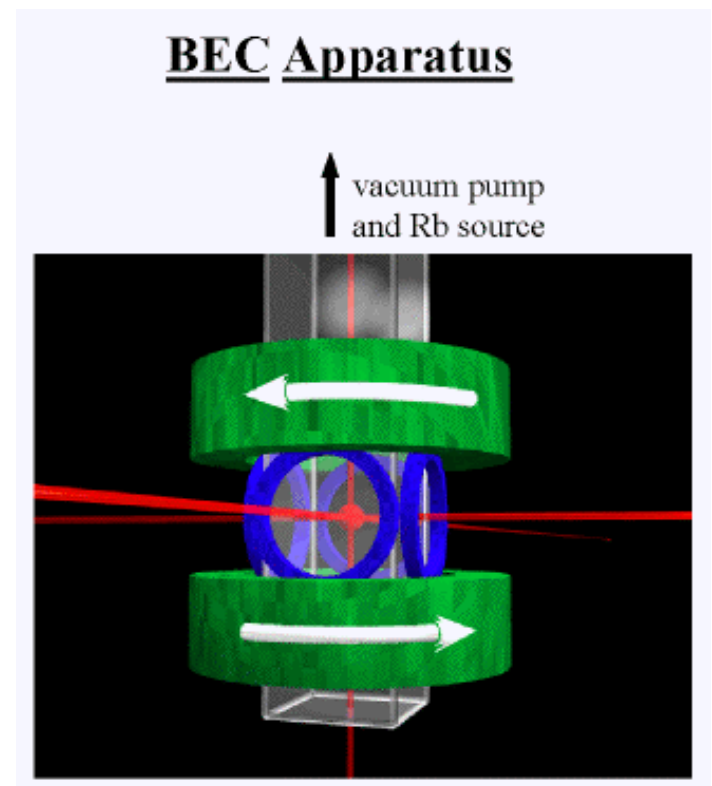
(4) XY model

$$H = -\sum_i \frac{1+\gamma}{2} \sigma_i^x \sigma_{i+1}^x + \frac{1-\gamma}{2} \sigma_i^y \sigma_{i+1}^y + \frac{\lambda}{2} \sigma_i^z$$
$$\lambda_c = \pm 1$$

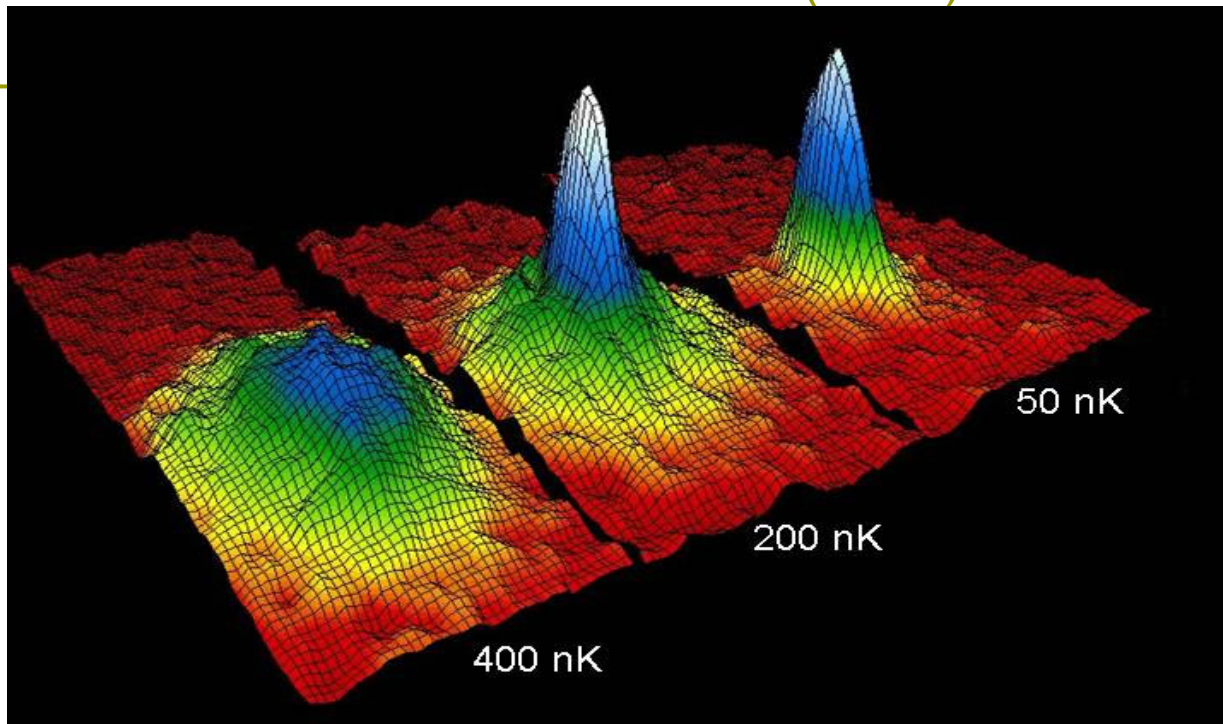
Its classical counterpart has a large d and an exponential decay of SP has been found.

(II) 冷原子系统——拾零

- ❑ Laser cooling (Stevens Chu, 1997 Nobel Prize in Physics)
- ❑ Evaporative cooling



First experimental realizations of Bose-Einstein condensates (BEC)



2001 Nobel prize in physics:

C. Wiemann: U. Colorado

E. Cornell: NIST

W. Ketterle: MIT

–Anderson et al.,
Science, 269 (1995),
198: JILA Group; Rb

–Davis et al., Phys.
Rev. Lett., 75 (1995),
3969: MIT Group; Rb

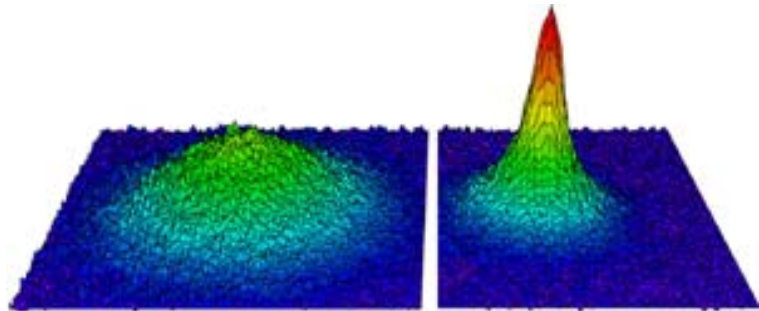
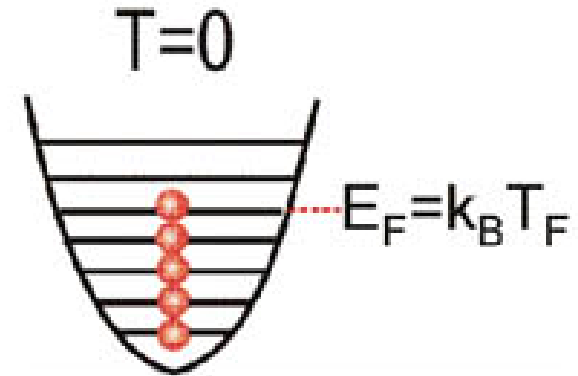
–Bradly et al., Phys.
Rev. Lett., 75 (1995),
1687, Rice Group; Li

Ultracold Fermi Gas (1999)

Ultracold molecules formed from an ultracold Fermi gas (2003)

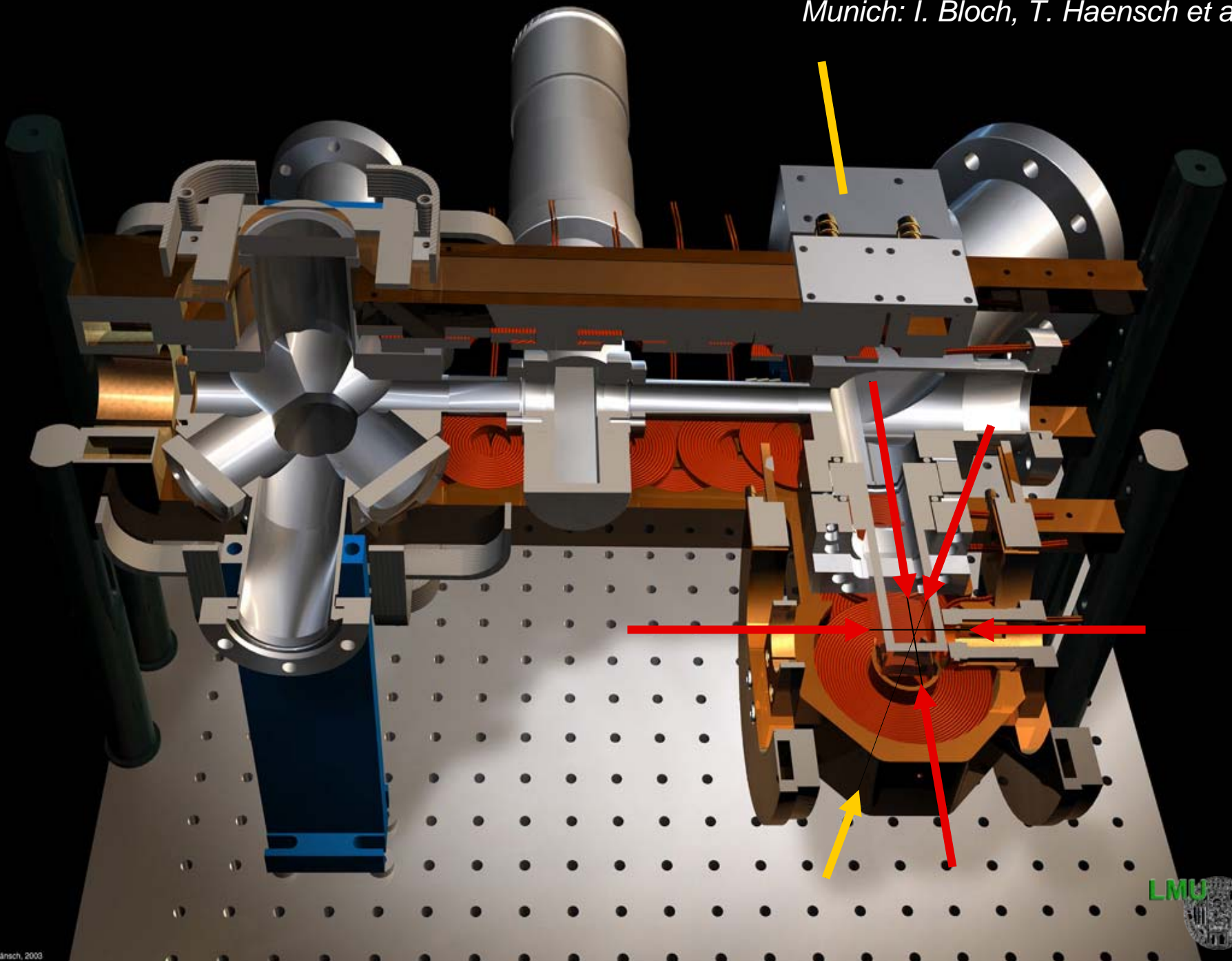
Molecular Bose-Einstein Condensate (2003)

Cold atoms with Fermi-Dirac statistics, 1999

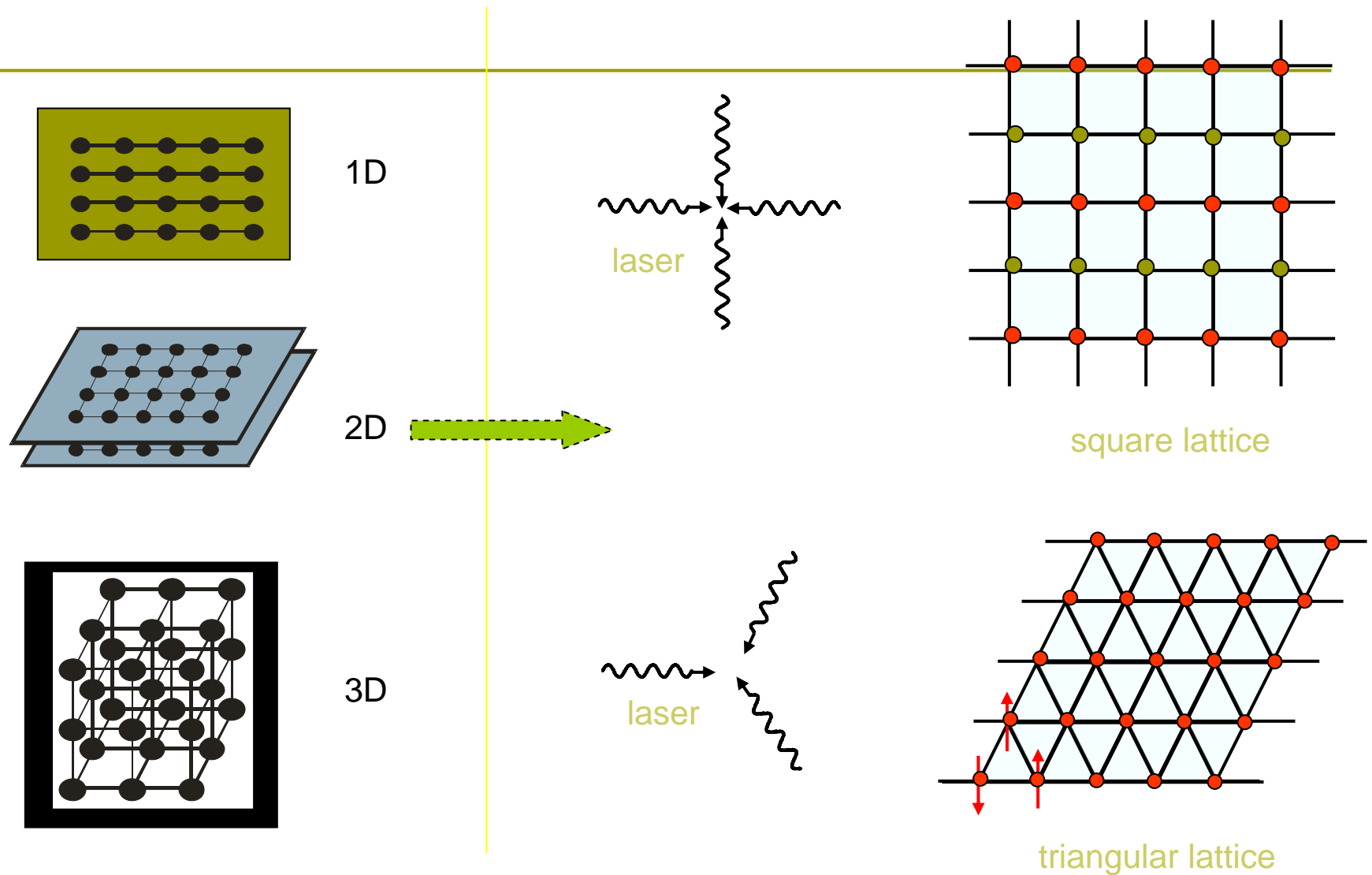


$$n(\varepsilon_i) = \frac{1}{e^{(\varepsilon_i - \mu)/k_B T} + 1}$$

Fermionic atom \rightarrow diatomic molecular BEC, 2003



Formation of 1D, 2D, 3D optical lattices



What can cold-atoms do?

- ❑ Quantum simulation of condensed-matter physics (electrons in periodic potentials, electrons in strong magnetic fields, superconductivity physics, spintronics)
- ❑ Exotic quantum materials (such as those with long-range dipolar interactions made from dipolar BECs, Bose-Fermi mixture, etc)
- ❑ Fundamental studies of ultracold physics, ultracold chemistry, and quantum physics (macroscopic quantum coherence, chemical reactions in the BEC regime)
- ❑ Quantum simulation of other physics areas, such as relativistic quantum mechanics, quantum field theory, nonlinear physics.
- ❑ Precision measurement, novel interferometry, better atomic clocks, novel atom devices...

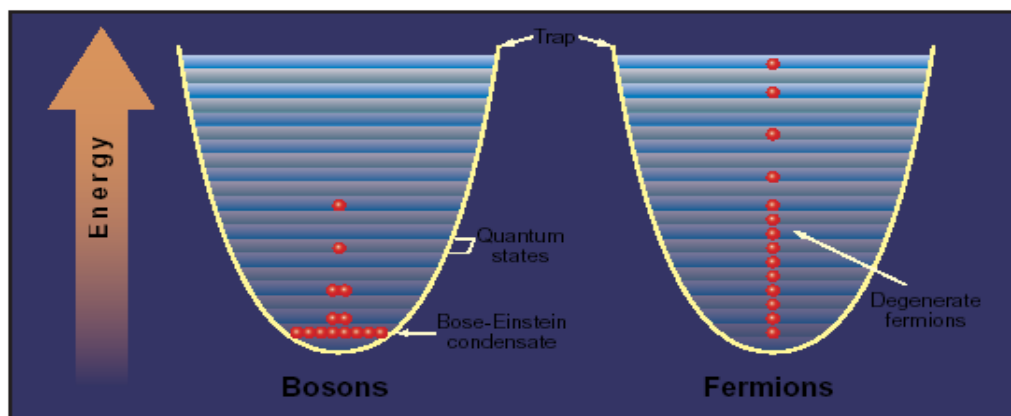
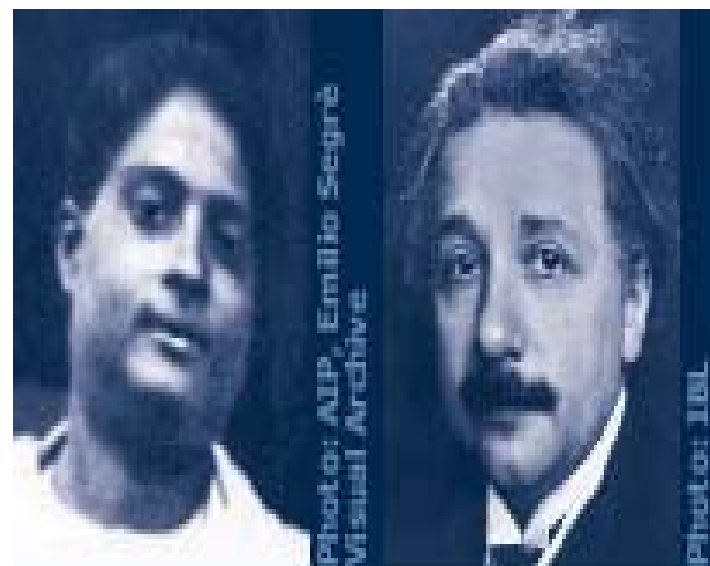
Example: Cold atoms in periodic optical potentials (optical lattices)

- Strongly correlated gas (e.g., Bose-Hubbard model, Fermi-Hubbard model)
- Bloch oscillations (extremely hard to observe in solid-state systems)
- Quasi-crystal
- Anderson localization
- ...

(II) 稀薄气体的玻色-爱因斯坦凝聚体(BEC)

1924

$$n(\varepsilon_i) = \frac{1}{e^{(\varepsilon_i - \mu)/k_B T} + 1}$$



Joiners and loners. Near absolute zero, identical bosons pile into the least energetic quantum state (left), whereas identical fermions stack into low-energy states one by one.

$$n_i = \frac{1}{e^{(\epsilon_i - \mu) / kT} - 1}$$

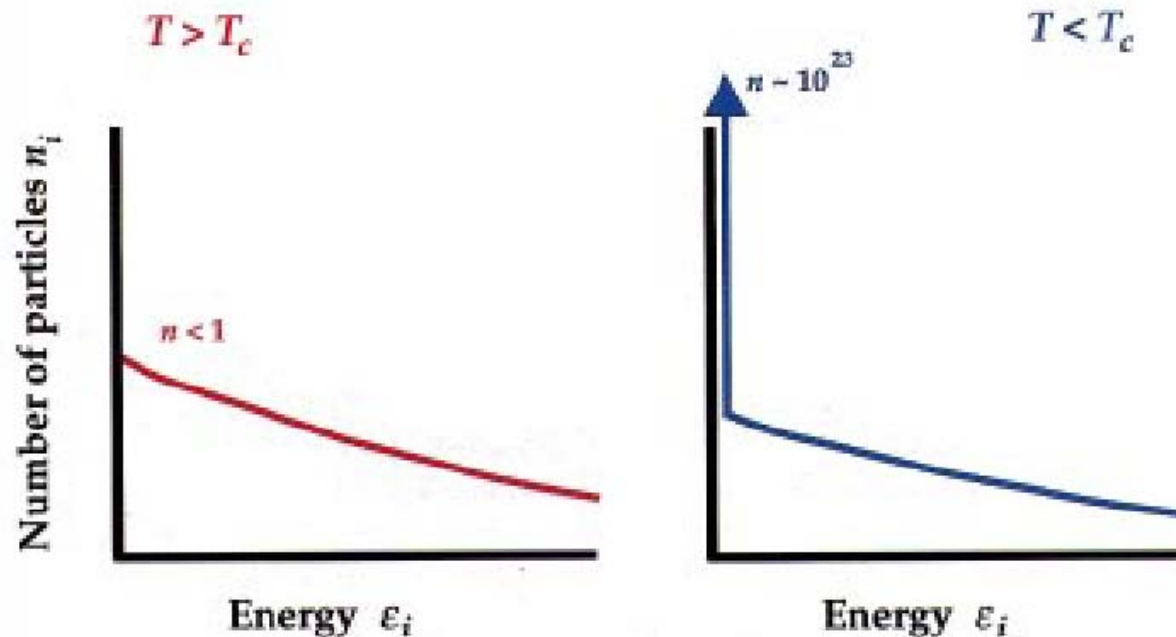
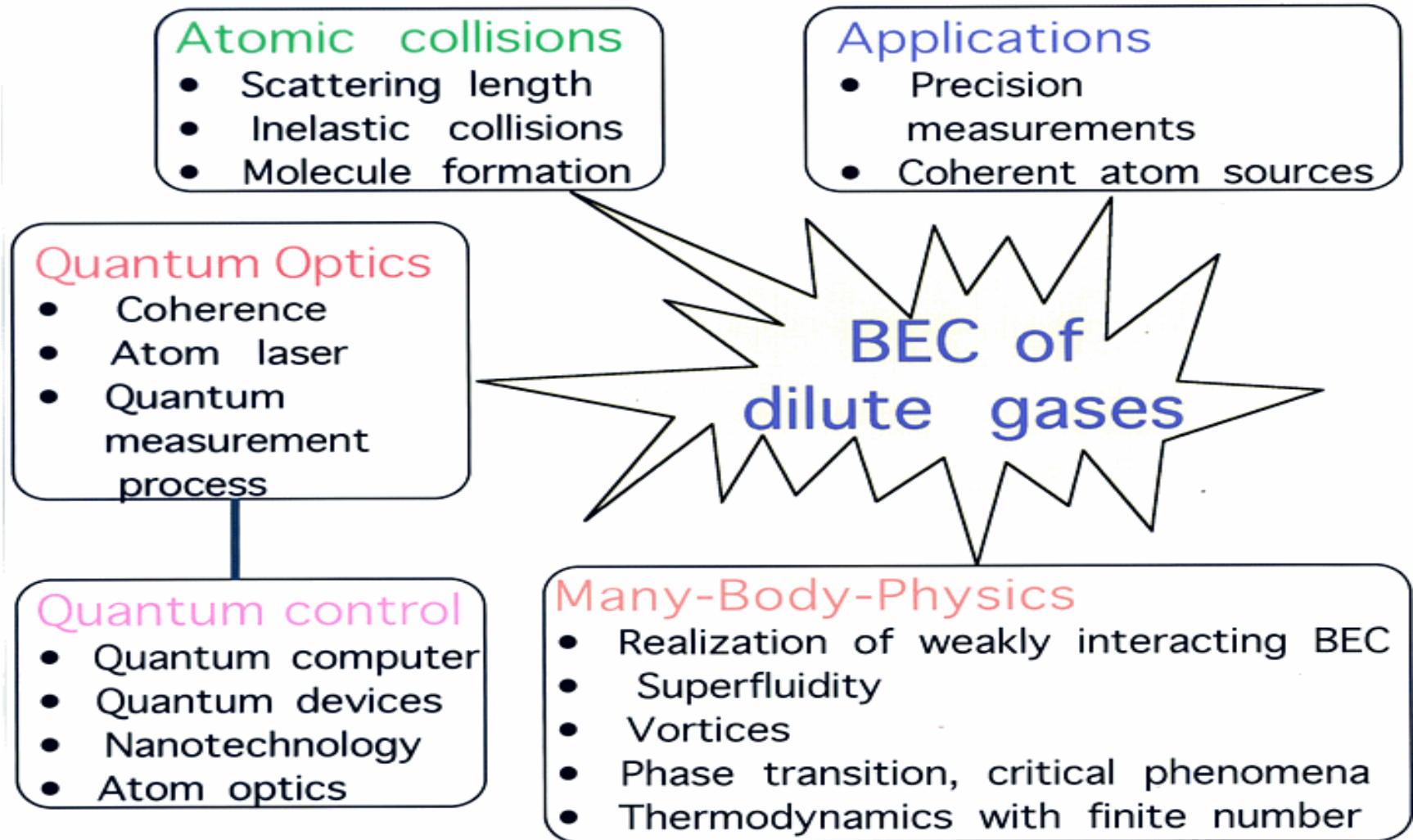
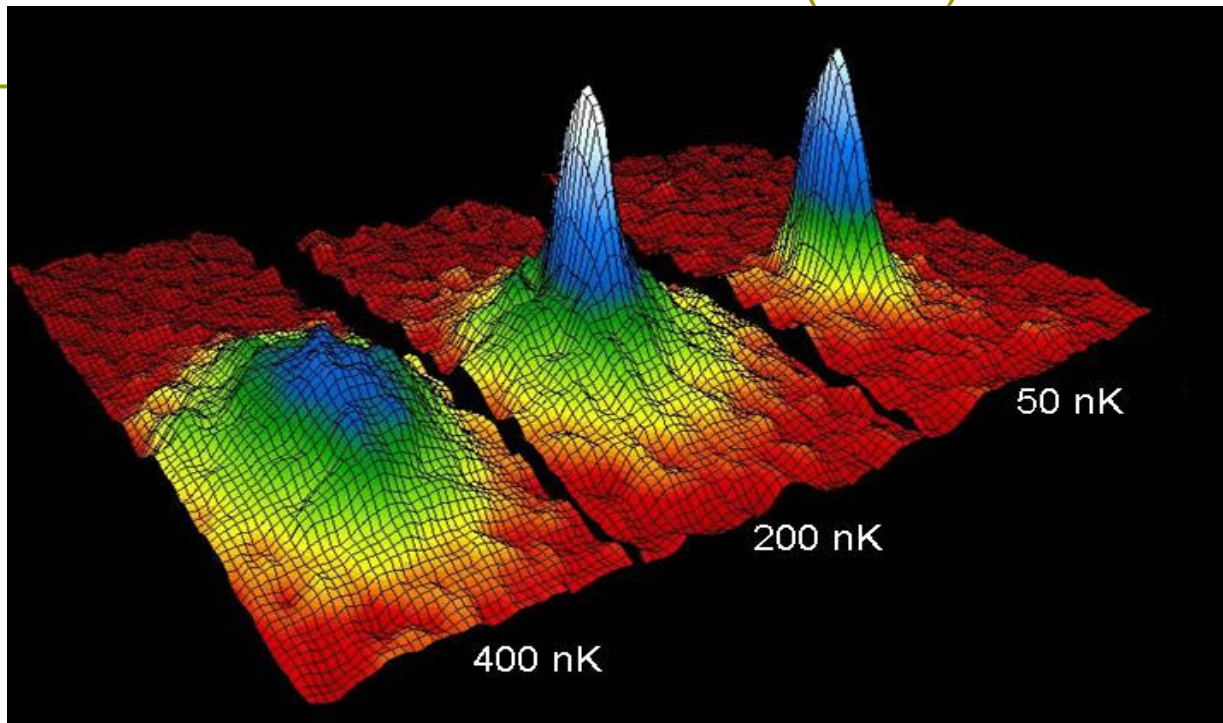


Fig. 2. Schematic diagram of the Bose-Einstein distribution for a system of particles at a temperature T . The formula shows the average number of particles n_i occupying a state i of energy ϵ_i . The parameter μ is the chemical potential, which is the energy required to add an additional particle to the system. The left frame depicts the general behavior of this distribution above the transition temperature T_c ; the right panel shows the macroscopic occupancy of the lowest state of the system when $T < T_c$.

Bose-Einstein condensates become an ultralow-temperature laboratory



First experimental realizations of Bose-Einstein condensates (BEC)



2001 Nobel prize in physics:

C. Wiemann: U. Colorado

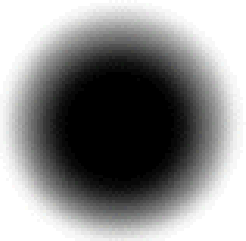
E. Cornell: NIST

W. Ketterle: MIT

–Anderson et al.,
Science, 269 (1995),
198: JILA Group; Rb

–Davis et al., Phys.
Rev. Lett., 75 (1995),
3969: MIT Group; Rb

–Bradly et al., Phys.
Rev. Lett., 75 (1995),
1687, Rice Group; Li



Some atoms in a BEC condensate

Typical parameters of BEC,
 Density $10^{11} \sim 10^{15} \text{ cm}^{-3}$
 Temperature $\text{nK} \sim \mu\text{K}$

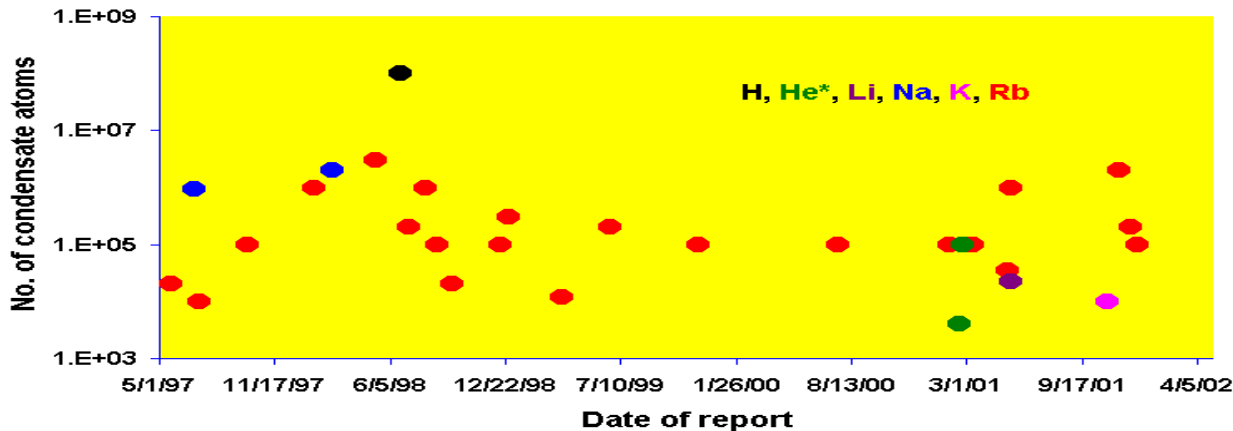
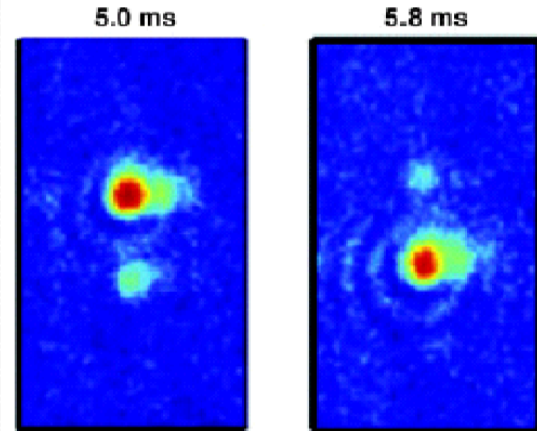
macroscopic quantum fluid phenomena
 interference
 tunnelling

The Nobel Prize in Physics 2001

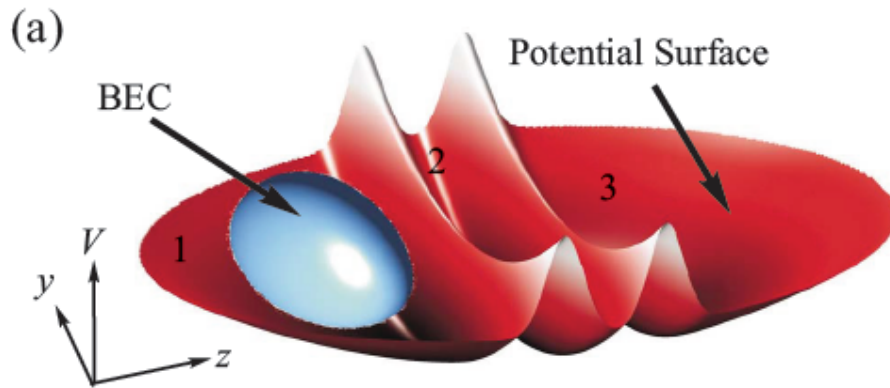


To the left, Ketterle's first interference pattern.

The interference pattern between two expanding condensates resembles that formed by throwing two stones into still water.



Example: Macroscopic quantum coherence: Matter transport without transit (Rab et al, 2008)



Tunneling rate from
well 1 to well 2 is Ω_{12}

Tunneling rate from
well 2 to well 3 is Ω_{23}

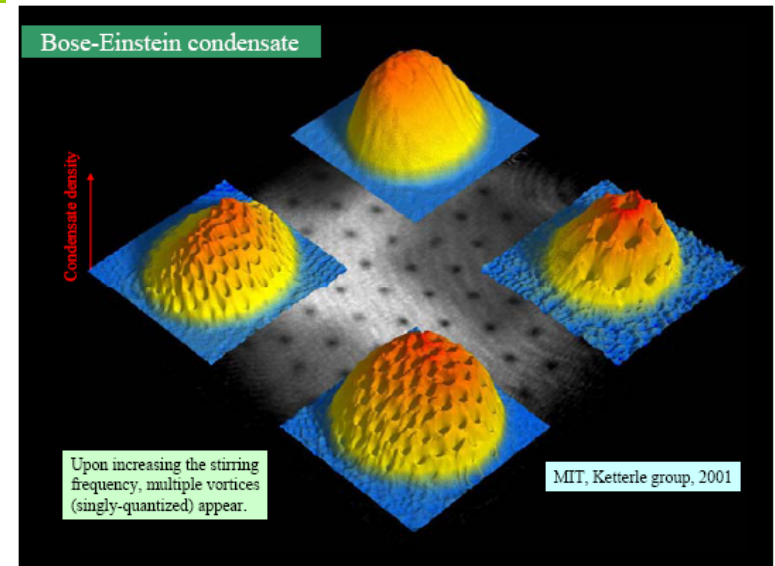
Assuming the same on-site
energy for the three wells,
the Hamiltonian is

$$H_{\text{eff}} = \hbar \begin{pmatrix} 0 & \Omega_{12} & 0 \\ \Omega_{12}^* & 0 & \Omega_{23} \\ 0 & \Omega_{23}^* & 0 \end{pmatrix}$$

More example: Cold-atom and Superconductivity:

Using rotating BEC to simulate superconductors in strong magnetic fields: formation of vortex lattices

From Abrikosov vortex lattice to vortex lattice in a rotating BEC



A.A. Abrikosov,
Nobel Prize 2003

BEC的基本特性

$T > T_c$, 热原子

$T < T_c$, 达到平衡态之后, 为BEC。

BEC的特点: 众多 (宏观数量) 粒子处于同一个宏观波函数所描述的状态, 可有超流 (超导) 性。

BEC的多体波函数描述:
$$\Psi_N(\mathbf{r}_1 \cdots \mathbf{r}_N) = \prod_{i=1}^N \chi_0(\mathbf{r}_i)$$

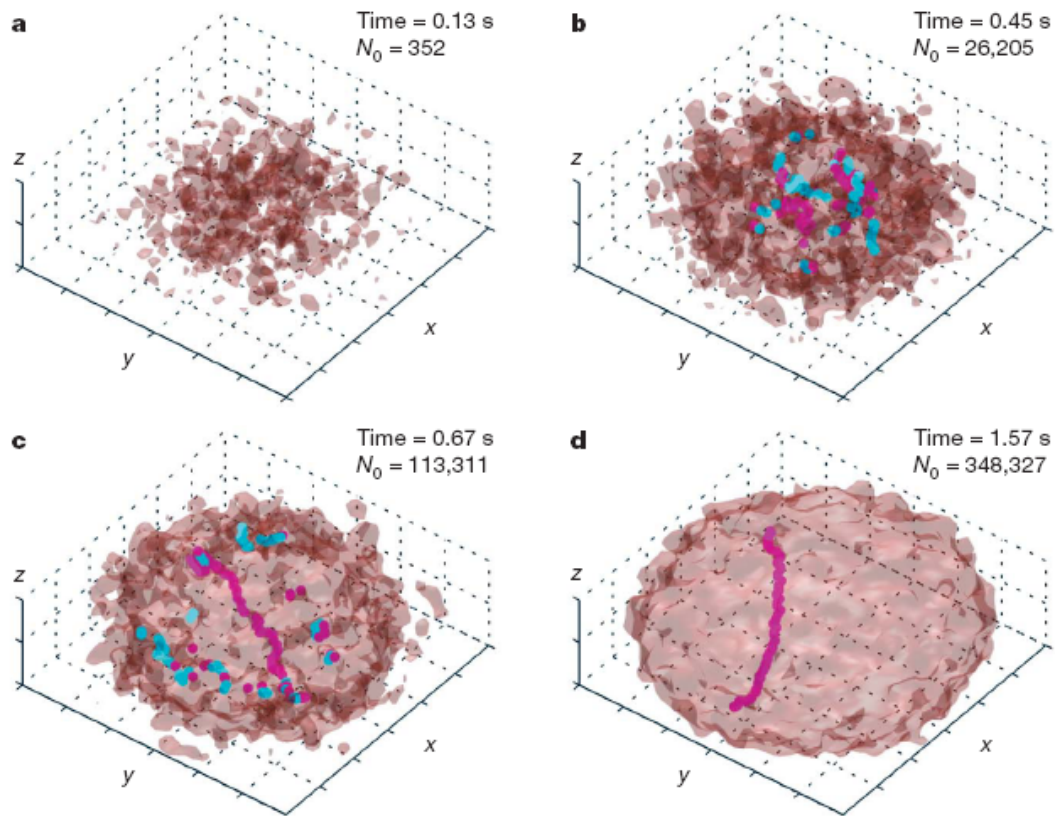
$$\Psi(\mathbf{r}t) \equiv \sqrt{N_0(t)} \chi_0(\mathbf{r}; t)$$

BEC的数学描述: Gross-Pitaevskii (GP)方程

$$-\frac{\hbar^2}{2m}\nabla^2\Psi(\mathbf{r}) + V_{ext}(\mathbf{r})\Psi(\mathbf{r}) + U_0|\Psi(\mathbf{r})|^2\Psi(\mathbf{r}) = \mu\Psi(\mathbf{r}),$$

BEC的形成过程如何描述？——对理论物理学家的挑战

实验



Nature 455, 948 (2008)

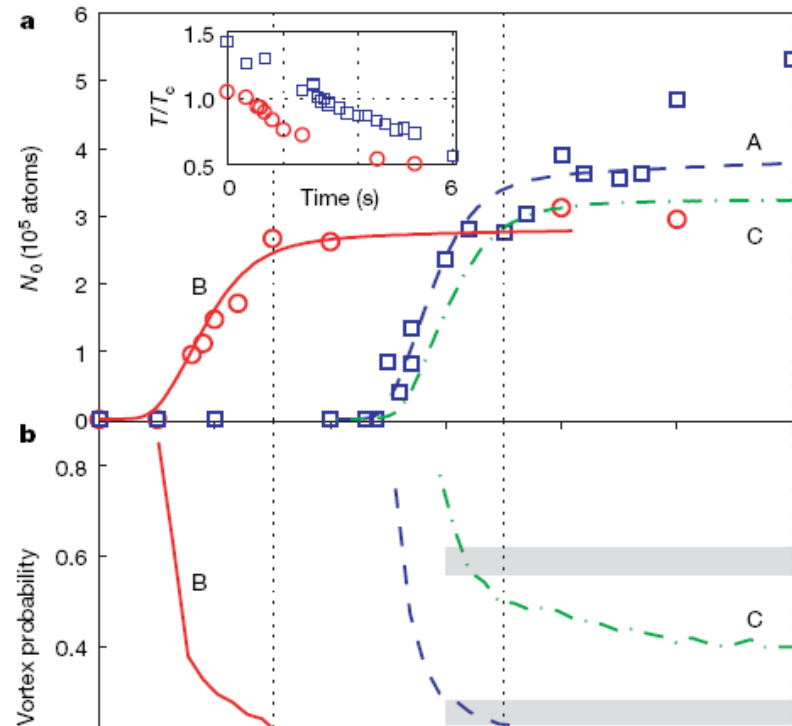


Figure 2 | Condensate formation and vorticity. **a**, Condensate number N_0 versus time. Blue squares (red circles) indicate experimental data for quench A (B), and lines indicate corresponding numerical simulations. The green dot-dashed line is the numerical result for the toroidal trap (quench C). Vertical dotted lines indicate the observation times for which experimental statistics are generated. Inset, experimentally measured temperatures for quenches A and B ($\tau_Q \approx 7$ s and 5 s, respectively). **b**, The probability of finding at least one vortex passing through the $z = 0$ plane plotted for all three simulated quenches. Grey regions indicate the experimental measurement range for each data set.

欢迎真心喜爱物理、不很介意物质利益得失的同学加入！

我们的研究方向：

(1) 复杂量子系统的各种性质：

- () 小量子系统的统计描述、热化
- () 环境导致的退相干效应
- () 量子相变
- () BEC的形成过程
- () 量子混沌

(2) 物理学中的一些基本问题：

- () 测量仪器的量子描述、量子力学基础
- () 描述远离平衡态系统的理论框架、统计力学基础
- () 质谱的解释、量子场论中无穷大出现的根源